



PERGAMON

International Journal of Multiphase Flow 24 (1998) 961–974

International Journal of
Multiphase
Flow

Wavespeed and volumetric fraction in core annular flow

A.C. Bannwart

Department of Energy, University of Campinas, UNICAMP Cx. P. 6122, 13083-970, Campinas, SP, Brazil

Received 29 January 1997; received in revised form 16 June 1998

Abstract

Kinematic wave theory is used to study the speed of interfacial waves observed in core annular flows of viscous oils with water. The theory provides a method for measuring the volume fraction of the core. The results obtained by this method are in very good agreement with experimental data. The model also confirms the observation that for oils lighter than water waves move slower than the core in upward flow, faster than the core in downward flow and at the same velocity of the core in horizontal flow. A general correlation for the core fraction in wavy core annular flows at low annulus-to-core viscosity ratio is proposed. © 1998 Elsevier Science Ltd. All rights reserved.

Keywords: Oil-water flow; Core annular flow; Volumetric concentration; Wavespeed; Slip ratio

1. Introduction

In many circumstances when two liquids of different viscosities flow together in a pipe, a core annular flow appears with the more viscous fluid in the core and the other in the annulus. An important practical application of this flow pattern has been found in the pipeline transportation of heavy oils by using water as lubricant.

As in gas–liquid annular flow, the interface in a core annular flow is usually wavy as a result of the complex interactions between the two phases. However the wave pattern in core annular flow is not a chaotic one. Due to the high viscosity of the core, the waves form a single pattern traveling at constant speed and wavelength depending on the flow rates, orientation and fluid properties. An interesting recent study on these waves in vertical core annular was made by Bai (1995). A detailed description of his experiment and the different flow patterns for upflow and downflow was presented earlier in the book by Joseph and Renardy (1993). In upward flow of

0301-9322/98/\$19.00 © 1998 Elsevier Science Ltd. All rights reserved.

PII: S0301-9322(98)00019-6

oil and water, the oil being lighter than water, he observed a pattern of interfacial waves that he called bamboo waves. In downward flow, the waves showed a different pattern of corkscrew waves. He measured the oil fraction and pressure drop in the tube and performed a numerical study of the wavy core annular flow.

In viscous oil–water flows, the high viscosity of the oil makes difficult the measurement of the oil fraction by closing-valves. Oils of thousands of cp, which are very common in industry, take a long time to flow and allow the separation of the water. It seems appropriate to develop alternative methods for the measurement of core fraction in such cases.

Wave phenomena are extremely important in two-phase flows because the flow parameters such as the local flow rates and pressures of each phase typically oscillate and these perturbations propagate through the flow field. The interface also oscillates and the combination of all these perturbations might cause growing disturbances and transition. Despite the complexity of the subject, two wave classes are commonly defined. If the flow is steady and a global equilibrium of forces can be assumed, the waves are described through the mass balance alone and are called kinematic waves [see for example Whitham (1974) or Wallis (1969), who prefer the term ‘continuity waves’]. The condition for these waves to occur is the existence of a relationship between the steady equilibrium flow rate of a substance and the area it occupies in the tube cross-section. This equilibrium flow rate is the direct outcome of the force balance. Thus, kinematic waves are first-order hyperbolic waves describing the propagation of velocity and concentration perturbations; they can be observed, for example, on the surface of liquid films flowing down a wall. Whenever the flow is unsteady or unstable, such as in the transition between two flow patterns, inertial effects must be taken into account and the corresponding perturbations are called dynamic waves; they are usually second-order hyperbolic waves and their celerities are called characteristics. This is the case, for example, of the Kelvin–Helmholtz instability waves used to analyze the stratified-to-intermittent gas-liquid transition in a horizontal duct (Wallis and Dobson 1973; Taitel and Dukler, 1976).

Both wave classes just described are usually present in an actual two-phase flow, and the condition that the kinematic wave velocity lies in between the highest and lowest characteristics is a celebrated stability criterion. If this condition is not obeyed and the kinematic wave moves faster than the highest characteristic, roll waves are seen at the interface (Whitham, 1974). None of this is observed in the core annular flows described in this paper. The viscosity of the core fluid is so much higher than the annulus that any dynamic effect on the interfacial wave is hardly noticeable. There seems to be a single wavespeed in a very stable flow. This is an indication that second order effects can be neglected and kinematic wave theory provides a good representation of the interfacial waves.

The speed of a kinematic wave is a well-defined quantity that can be related to the fraction of the core. This provides a method for the measurement of volumetric fraction. In the present work, the proposed technique is applied to measurements of wavespeed for a viscous oil-water system flowing in a 2.25 cm ID horizontal tube and to the vertical flow measurements made by Bai (1995) as well. A general correlation for the volumetric fraction of the core, valid at low annulus-to-core viscosity ratios, is proposed.

2. Wave model

For a two-phase incompressible flow, the speed of kinematic waves, a , can be defined by (Wallis, 1969)

$$a = \left(\frac{\partial J_1}{\partial \varepsilon_1} \right)_J \quad (1)$$

where J_1 is the superficial velocity of the fluid at the core, ε_1 is the fraction of the tube occupied by this fluid, $J = J_1 + J_2$ is the total superficial velocity and J_2 is the superficial velocity of fluid at the annulus. Eq. (1) can also be written as

$$a = \left(\frac{\partial J_2}{\partial \varepsilon_2} \right)_J = - \left(\frac{\partial J_2}{\partial \varepsilon_1} \right)_J, \quad (2)$$

where the fraction occupied by fluid 2 is $\varepsilon_2 = 1 - \varepsilon_1$. An important quantity in what follows is the ratio, s , which means the ratio between the actual velocities of the phases i.e.

$$s = \frac{U_1}{U_2} = \frac{J_1(1 - \varepsilon_1)}{\varepsilon_1 J_2}, \quad (3)$$

where U_1 is the average velocity of the fluid at the core and U_2 is the average velocity for the fluid at the annulus. The slip ratio is then equivalent to the holdup ratio introduced by Charles et al. (1961). Eq. (1) suggests working with a triangular relationship of the form $f(\varepsilon_1, J_1, J) = 0$ or equivalently $g(\varepsilon_1, J_1, J_2) = 0$. Such relationships can be easily derived for some simple core annular flows as shown next.

3. Horizontal flow

Consider a perfect core annular flow, which is a fully developed laminar two-phase flow having a smooth axisymmetric interface and density match. The triangular relationship can be derived eliminating the pressure gradient from the solution of the momentum equations. For small viscosity ratio ($\mu_2/\mu_1 \rightarrow 0$) this gives

$$J_1(1 - \varepsilon_1) - s_o J_2 \varepsilon_1 = 0 \quad (4)$$

where $s_o = 2$. It can be concluded from (3) that the constant s_o corresponds to the slip ratio for perfect core annular flow.

It can be assumed that (4) is also valid for horizontal core annular flow with a wavy interface, but a different value for the constant s_o has to be determined from experiment. In fact, for a wavy interface neither the velocity profile in the annulus is a simple parabolic distribution nor the streamlines are axially oriented. A substantial amount of the fluid in the annulus typically forms an eddy in the gap between two wave crests while the amount left flows through a much smaller annular space between the wave crest and the wall (Feng et al., 1995). Since the eddy moves forward essentially at the same velocity of the core, it can be

expected that $s_o < 2$ for a wavy interface. If turbulence is present in the annulus (Oliemans et al., 1986), the velocity profile in the annulus gets flatter and s_o can be considerably less than 2.

The speed of kinematic waves can be obtained by applying (1) and (2)–(4). This gives

$$a = \frac{(J_1 + s_o J_2)^2}{s_o J} \tag{5}$$

In terms of the velocities J , U_1 and U_2 the wavespeed can be expressed, respectively, as

$$a = J \left[1 - \frac{(\sqrt{s_o} - 1)(J_1/\sqrt{s_o} - J_2)}{J} \right]^2, \tag{6}$$

$$a = U_1 \frac{J_1/s_o + J_2}{J}, \tag{7}$$

$$a = U_2 \frac{J_1 + s_o J_2}{J} \tag{8}$$

and from these one concludes [assuming $J_1 \geq \sqrt{s_o} J_2$ in (6)]

$$\begin{cases} U_1 \leq J \leq a \leq U_2 & s_o \leq 1 \\ U_1 > J > a > U_2 & s_o > 1 \end{cases} \tag{9}$$

3.1. Experimental set-up

The author ran experiments using a viscous oil and water at room temperatures in a horizontal tube at various flow rates of each fluid. The oil was the no. 6 fuel oil (density = 0.989 g/cm³, viscosity = 27 poise). The experimental apparatus is shown in Fig. 1. From a 1 m³ separator tank oil was drawn by a progressive cavity pump (Moyno) with variable speed and the flow rate was measured through a direct mass flowmeter (Micro

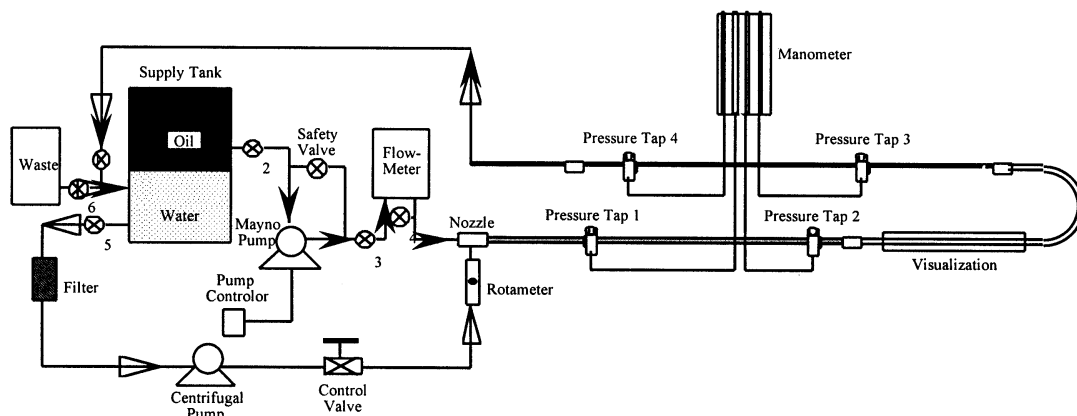


Fig. 1. Diagram of the experimental set-up.

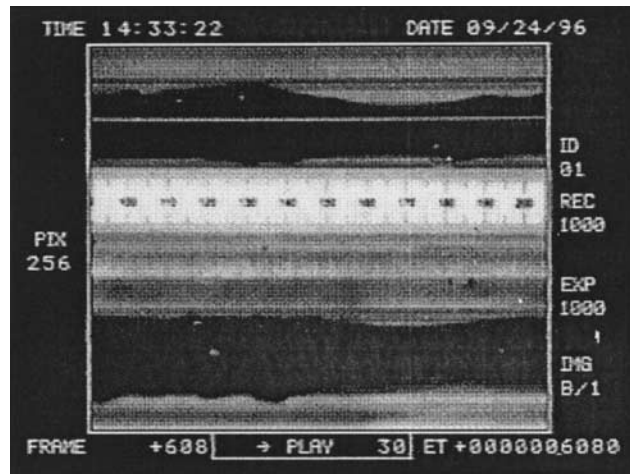


Fig. 2. Example of photograph obtained from high-speed imaging, showing the top and side views of a core-annular flow of viscous oil and water inside a 2.25 cm horizontal tube (the straight white line is the top view of the scale shown).

Motion). Water was drawn from the bottom of the tank by a centrifugal pump, filtered and measured through a rotameter. The injection nozzle was a simple device having a central tube inlet for oil and a surrounding shell for water. The oil to water input ratio was varied from 1 to 11.

The test section for wavespeed measurement was a glass J-shaped tube 2.25 cm ID. The wavespeed was measured with a Kodak EktaPro EM high-speed camera. The procedure consisted in running the flow at a specified pair of flow rates for 15 min then making three readings of both water and oil rates. A 5 s movie of the flow in the test section was recorded during the second of those readings. Fig. 2 shows an example of image provided by the high-speed camera. Thanks to a mirror placed just above the test section at a 45-degree angle, it was possible to catch both top and side views of the flow simultaneously as indicated. A pattern consisting of asymmetric bamboo waves moving at constant speed was observed for each pair of flow rates. The core annular flow was slightly off-centered to the upper part of the tube. Fig. 2 also shows the scale added to the movie, so the wavespeed was determined by measuring the distance traveled by a wave crest between two marks on the scale and the correspondent elapsed time (shown at the bottom right of each frame). Either top or side view could be used for that purpose. Four determinations of wavespeed were made for each run. Before setting the next pair of flow rates the system was run with pure water until the pressure drop through the entry and exit steel tubes were low enough so as to make sure that the tubes were clean from the fouling action by the no. 6 fuel oil.

Table 1 shows the measured wavespeed for each pair of flow rates used in the experiments. A plot of these data in the form a/J_2 vs J_1/J_2 is shown in Fig. 3. In order to determine the parameter s_0 , a standard least-squares technique was applied to the total deviation function

$$E = \sum_i^{\text{data}} \left[\left(\frac{a}{J_2} \right)_{\text{th}} - \left(\frac{a}{J_2} \right)_i \right]^2, \quad (10)$$

Table 1

Experimental data on wavespeed and superficial velocities for a core annular flow of oil-water inside a 2.25 cm ID horizontal tube

Point no.	Temp. (°C)	J_1 (m/s)	J_2 (m/s)	J (m/s)	a (m/s)
1	21.2	0.3890	0.2710	0.6600	0.6700
2	21.5	0.3723	0.2206	0.5929	0.5785
3	21.8	0.3658	0.1575	0.5233	0.5077
4	21.9	0.3042	0.0945	0.3987	0.4267
5	22.9	0.3127	0.0599	0.3726	0.3387
6	22.4	0.5454	0.2647	0.8101	0.8043
7	22.4	0.4937	0.2143	0.7080	0.6907
9	22.8	0.4774	0.1575	0.6349	0.6296
10	22.3	0.4833	0.0945	0.5778	0.5895
11	21.5	0.4505	0.0662	0.5167	0.5328
12	20.5	0.6316	0.2678	0.8994	0.9094
13	20.6	0.6038	0.2206	0.8244	0.8388
14	20.6	0.6156	0.1891	0.8047	0.8084
15	20.5	0.6093	0.1166	0.7259	0.7533
16	21.9	0.6078	0.0599	0.6677	0.6899
17	21.4	0.3033	0.2804	0.5837	0.6278
18	21.6	0.3093	0.2237	0.5330	0.5312
19	21.7	0.2914	0.1670	0.4584	0.4626
20	22.1	0.2872	0.0945	0.3817	0.4158
21	20.5	0.2554	0.0347	0.2901	0.3051
22	20.9	0.4560	0.2836	0.7396	0.7643
23	21.5	0.4440	0.2269	0.6709	0.6534
24	22.4	0.4291	0.1607	0.5898	0.5822
25	24.9	0.4180	0.0977	0.5157	0.4964
26	25.7	0.4329	0.0378	0.4707	0.4869
27	26.9	0.5683	0.2741	0.8424	0.8386
28	27.0	0.5813	0.2237	0.8050	0.7741
29	27.0	0.5695	0.1575	0.7270	0.7239
30	26.1	0.5660	0.0882	0.6542	0.6328
31	25.6	0.5599	0.0599	0.6198	0.6303

where $(a/J_2)_{th}$ is the theoretical ratio determined from (5) and $(a/J_2)_i$ is the experimental value. Using the command FindMinimum of the software Mathematica was minimized E with respect to s_o to obtain

$$s_o = 1, \quad (11)$$

which means that in horizontal flow both fluids at the core and annulus are flowing at the same velocity. This velocity is also the velocity of the waves and corresponds to the superficial velocity of the mixture J [see (5)–(8)]. The solid line in Fig. 3 represents the plot of (5) for $s_o = 1$.

A few comments can be made about this all-important result. First, the low spread of the data around the theoretical curve in Fig. 3 shows that (5) is no doubt a very good representation of the wavespeed data; this is an indication that the model describes correctly the interfacial waves. Second, the result $a = J$ from (6) is also an indication of the plausibility

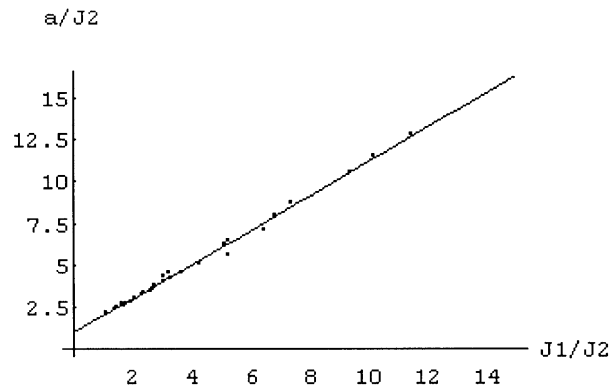


Fig. 3. Plot of a/J_2 vs J_1/J_2 for core annular flow of oil-water inside a 2.25 cm ID horizontal tube. Data are from Table 1; the solid line represents (5) with $s_o = 1$.

of the wave model proposed, because that result could be anticipated by the direct plot of a vs J shown in Fig. 4. Third, it can be concluded from (7) that the wave is moving at the same speed of the core, a physically attractive outcome in view of the high viscosity of the core. Fourth, (11) shows the strong mixing effect of the interfacial waves and, possibly, turbulence. Finally, the result seems to confirm the expectation that in the absence of a body force in the direction of the flow, there is no net drag on the highly viscous core, thus no velocity difference between the phases. Oliemans et al. (1986) determined water holdups from photographs. The slip ratio correspondent to their holdup correlation was in the range 1.08–1.16. Although their method can be somewhat inaccurate because of the asymmetry of the flow, that their measurement compares favorably with the present result.

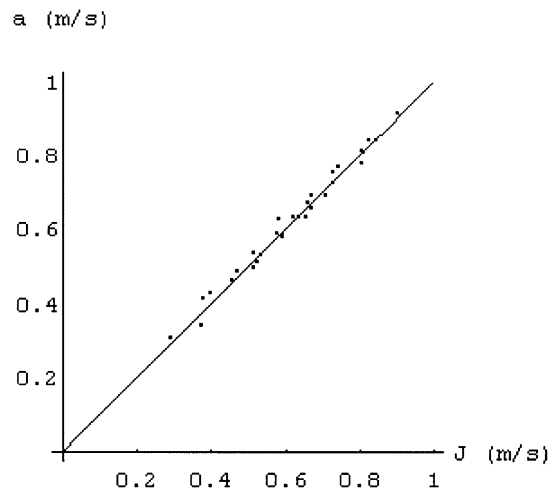


Fig. 4. Direct plot of wavespeed a vs mixture superficial velocity J for core annular flow of viscous oil-water inside a 2.25 cm ID horizontal tube. Data are from Table 1. The conclusion $a = J$ (solid line) can thus be deduced directly from the data and confirms (11).

4. Vertical flow

For vertical core annular flow with a smooth interface, but different densities (4) has to be modified to

$$J_1(1 - \varepsilon_1) - s_o J_2 \varepsilon_1 - V_{\text{ref}} F(\varepsilon_1) = 0, \quad (12)$$

where $s_o = 2$ and V_{ref} is a reference velocity defined by

$$V_{\text{ref}} = \frac{(\rho_1 - \rho_2) g_z D^2}{16\mu_2}, \quad (13)$$

where ρ_1 and ρ_2 are the densities of the fluids at the core and annulus, respectively, μ_2 is the absolute viscosity of the fluid at the annulus, D is the tube diameter and g_z is the component of gravity acceleration in the direction of the flow (negative for upflow, positive for down flow). Thus, $V_{\text{ref}} > 0$ for either upflow of fluid 1 lighter than fluid 2 or downflow of fluid 1 heavier than fluid 2; otherwise $V_{\text{ref}} < 0$. The function $F(\varepsilon_1)$ is given by

$$F(\varepsilon_1) = -\varepsilon_1^2 [2(1 - \varepsilon_1) + (1 + \varepsilon_1) \ln \varepsilon_1]. \quad (14)$$

Comparing (12) and (3) one obtains the slip ratio s as

$$s = s_o + \frac{F(\varepsilon_1)}{J_2^* \varepsilon_1} \quad (15)$$

where

$$J_2^* = \frac{J_2}{V_{\text{ref}}}. \quad (16)$$

It can be shown from (13)–(15) that $s > s_o$ for $J_2^* > 0$ which corresponds to upflow of lighter fluid 1 or downflow of heavier fluid 1; otherwise $s < s_o$.

An excellent approximation for the function $F(\varepsilon_1)$ given by (14) is the expression $0.8\varepsilon_1^2(1 - \varepsilon_1)^{4.5}$. This suggests that for a wavy interface

$$F(\varepsilon_1) = k\varepsilon_1^2(1 - \varepsilon_1)^n, \quad (17)$$

where the parameters k and n are to be determined from experiments. Eq. (12) then becomes

$$J_1(1 - \varepsilon_1) - s_o J_2 \varepsilon_1 - k V_{\text{ref}} \varepsilon_1^2 (1 - \varepsilon_1)^n = 0 \quad (18)$$

and the correspondent speed of the kinematic wave is given by

$$a = \frac{J_1 + s_o J_2 + k V_{\text{ref}} \varepsilon_1 (1 - \varepsilon_1)^{n-1} [2(1 - \varepsilon_1) - n\varepsilon_1]}{1 + (s_o - 1)\varepsilon_1}. \quad (19)$$

The above relation can be reduced to (5) when $V_{\text{ref}} = 0$ (horizontal flow).

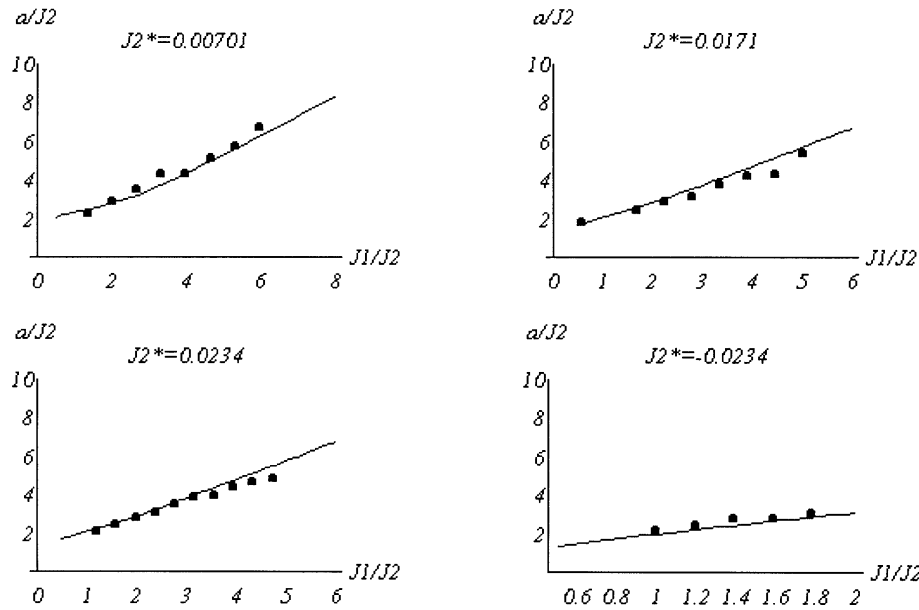


Fig. 5. Plot of a/J_2 vs J_1/J_2 at various J_2^* for core annular flow of motor oil–water inside a 0.9525 cm ID vertical tube. Data are from Table 2; in each graph the solid line represents (19) with parameters given by (11) and (20). ($J_2^* > 0$ for upflow, $J_2^* < 0$ for downflow).

4.1. Experimental data

Bai (1995) reports wavespeed and holdup measurements for vertical flow of Motor Oil (density = 0.905 g/cm³; viscosity = 6 poise) and water at room temperatures inside a 0.9525 cm ID tube. Thus $|V_{ref}| \cong 5$ m/s. The input ratio was in the range $0.6 < J_1/J_2 < 8$. He observed axisymmetric bamboo waves for upflow and corkscrew waves for downflow. The wavespeed data is reproduced in Table 2.

4.2. Results and comments

Consistently with the horizontal flow result, it can be assumed that $s_o = 1$ and the data from Table 2 used to determine k and n . For this purpose, the total deviation function E was defined as in (10) and replaced $(a/J_2)_{th}$ using (19). With the core fraction ε_1 determined from (18), minimized E with respect to k and n , a task easily performed with Mathematica. The result is

$$k = 0.0194 \quad n = 1.75. \tag{20}$$

If n is assumed to be integer then the best choice is the set $k = 0.0223$, $n = 2$.

Fig. 5 shows the comparison between the waveXspeed as calculated from (19) and measured values from Table 2 for upflow and downflow. The good quality of the fit is clear.

A comparison between the volumetric fraction obtained from (18) and the measurements made by Bai (1995) is shown in Fig. 6. He measured the core fraction for a motor oil–water

Table 2

Experimental data on wavespeed and superficial velocities for a core annular flow of oil–water inside a 0.9525 cm ID vertical tube (extracted from Bai, 1995)

Point no.	Orientation	J_1 (m/s)	J_2 (m/s)	J (m/s)	a (m/s)
1	upflow	0.0469	0.0351	0.0820	0.0812
2	upflow	0.0699	0.0351	0.1050	0.1025
3	upflow	0.0930	0.0351	0.1281	0.1242
4	upflow	0.1160	0.0351	0.1511	0.1529
5	upflow	0.1384	0.0351	0.1735	0.1549
6	upflow	0.1620	0.0351	0.1971	0.1817
7	upflow	0.1850	0.0351	0.2201	0.2032
8	upflow	0.2080	0.0351	0.2431	0.2381
9	upflow	0.0469	0.0468	0.0937	0.0997
10	upflow	0.0930	0.0468	0.1398	0.1391
11	upflow	0.1390	0.0468	0.1858	0.1703
12	upflow	0.1850	0.0468	0.2318	0.2100
13	upflow	0.2311	0.0468	0.2779	0.2495
14	upflow	0.2771	0.0468	0.3239	0.2936
15	upflow	0.3231	0.0468	0.3699	0.3259
16	upflow	0.3692	0.0468	0.4160	0.4107
17	upflow	0.0483	0.0854	0.1337	0.1619
18	upflow	0.1430	0.0854	0.2284	0.2132
19	upflow	0.1904	0.0854	0.2758	0.2509
20	upflow	0.2377	0.0854	0.3231	0.2757
21	upflow	0.2851	0.0854	0.3705	0.3306
22	upflow	0.3325	0.0854	0.4179	0.3658
23	upflow	0.3798	0.0854	0.4652	0.3767
24	upflow	0.4272	0.0854	0.5126	0.4681
25	upflow	0.1390	0.1173	0.2563	0.2521
26	upflow	0.1850	0.1173	0.3023	0.2938
27	upflow	0.2311	0.1173	0.3484	0.3400
28	upflow	0.2771	0.1173	0.3944	0.3715
29	upflow	0.3232	0.1173	0.4405	0.4173
30	upflow	0.3692	0.1173	0.4865	0.4573
31	upflow	0.4153	0.1173	0.5326	0.4698
32	upflow	0.4613	0.1173	0.5786	0.5215
33	upflow	0.5073	0.1173	0.6246	0.5580
34	upflow	0.5534	0.1173	0.6707	0.5774
35	downflow	0.1022	0.0351	0.1373	0.1839
36	downflow	0.1454	0.0468	0.1922	0.1949
37	downflow	0.1503	0.0468	0.1971	0.2130
38	downflow	0.1638	0.0468	0.2106	0.2231
39	downflow	0.1160	0.1173	0.2333	0.2595
40	downflow	0.1390	0.1173	0.2563	0.2964
41	downflow	0.1620	0.1173	0.2793	0.3302
42	downflow	0.1850	0.1173	0.3023	0.3352
43	downflow	0.2081	0.1173	0.3254	0.3714

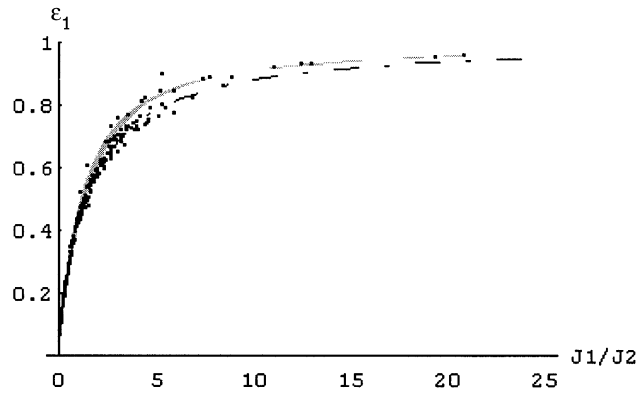


Fig. 6. Plot of ε_1 vs J_1/J_2 for core annular upflow of oil–water inside a 0.9525 cm ID vertical tube. The points stand for Bai’s experimental data; the dash-dot line corresponds to Bai’s experimental correlation (21) and the shaded area corresponds to (18) in the experimental range $0.007 \leq J_2^* \leq 0.0234$.

flow by the holdup valves method in the range $0.1 < J_1/J_2 < 20$, $0.007 < J_2^* < 0.1$ and expressed the results for upflow by an average holdup ratio of 1.39. This corresponds to [see (3)]

$$\varepsilon_{1,\text{exp}} = \frac{J_1/J_2}{J_1/J_2 + 1.39}, \tag{21}$$

which is also shown in Fig. 6. The shaded region represents (18) for $0.007 < J_2^* < 0.0234$ which corresponds to the water flow rate interval from Table 2. The agreement between experimental holdup values and the calculations using (18) can be considered very good. The difference between the holdup calculated from (18) and (21) is less than 10%.

A few outcomes of the correlation (18) deserve discussion. Fig. 7 shows a plot of the slip ratio as given by (15). It indicates as expected that fluid 1 moves faster than fluid 2 for $J_2^* > 0$,

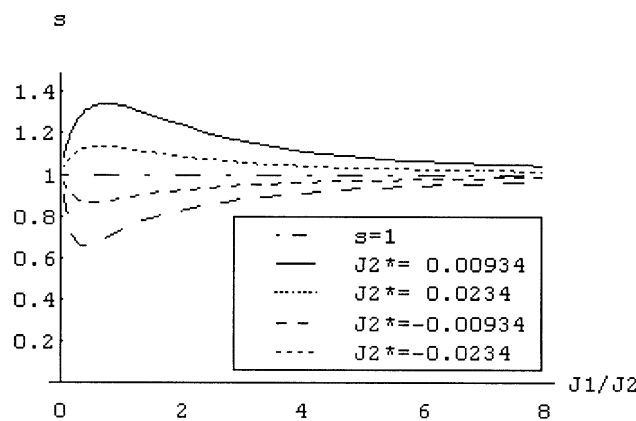


Fig. 7. Plot of s vs J_1/J_2 at various J_2^* according to (15). The curve $s = 1$ corresponds to horizontal flow.

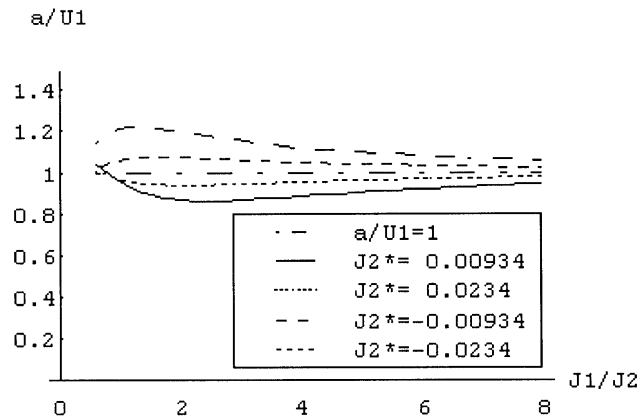


Fig. 8. Plot of a/U_1 vs J_1/J_2 at various J_2^* from (18) and (19).

which means upward flow with fluid 1 lighter than fluid 2 (or downward flow of heavier fluid 1). This figure also shows that one should approach the horizontal flow limit for high flowrates, when body forces become negligible.

Another interesting result is shown in Fig. 8, which compares the wavespeed to the core velocity. These quantities are determined from (18) and (19). For upflow and fluid 1 lighter than fluid 2 the wavespeed is lower than the core velocity in the range of input ratio for which core annular flow is usually observed. The same situation was observed by Bai (1995). This result is physically attractive since the fluid at the annulus is moving at a lower velocity than the core and thus must exert a drag on it. A similar explanation holds in the case of downward flow and fluid 1 lighter than fluid 2, when the wavespeed is higher than the core velocity and fluid 2 is moving faster than fluid 1. This is also confirmed by the measurements made by Bai. Thus the drag force on the core must be in balance with the flotation force. It is precisely this balance that is described by (18).

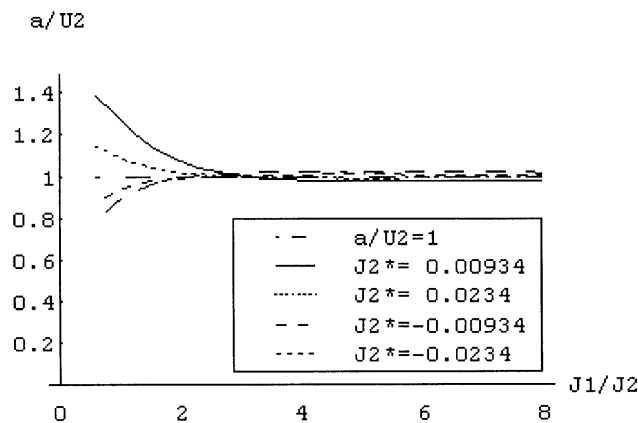


Fig. 9. Plot of a/U_2 vs J_1/J_2 at various J_2^* from (18) and (19).

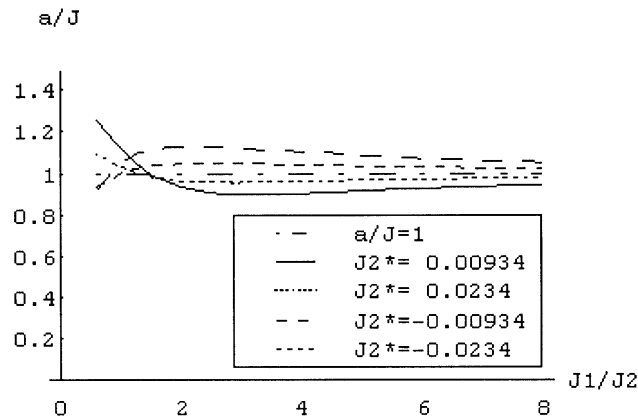


Fig. 10. Plot of a/J vs J_1/J_2 at various J_2^* from (18) and (19).

Fig. 9 shows that for oil-to-water input ratios greater than about 2 the annulus flow has nearly the same velocity of the wave. This is also expectable because the annulus gets thin in that condition. Finally, it is useful to compare the wavespeed to the total superficial velocity J . This is done in Fig. 10, which shows generally the same trends of Fig. 8.

5. Concluding remarks

Kinematic wave theory is a very useful tool to understand interfacial waves in core-annular flows with a viscous core, a situation of great practical interest. It was shown that the theory not only provides information on the wavespeed but also on the slip ratio and volumetric fraction of the core. Thus a technique for determining the core fraction from wavespeed measurements was developed whose results are in very good agreement with direct holdup measurements. Using data of oil–water systems (oil lighter than water) in both horizontal and vertical flow a general correlation was developed for the volumetric fraction of the core in core-annular flows at low viscosity ratio. The correlation, which is given by (18), includes the effect of fluid properties and can be applied to upward, downward and horizontal flows. It can, of course, be improved by additional data from other fluid systems, pipe inclination and range of flow parameters. However, in its present form, it is capable of representing some important phenomena reported in the literature.

Acknowledgements

This study was developed during my visit to the Department of Aerospace Engineering and Mechanics of the University of Minnesota, where I worked at Professor D. D. Joseph's lab. My gratitude is also directed to the Department of Energy of the University of Campinas (UNICAMP) and to FAPESP, Brazil, for the financial support provided. Taehwan Ko collaborated during the experiments described in Section 3.

References

- Bai, R., 1995. Traveling waves in a high viscosity ratio and axisymmetric core annular flow. PhD thesis, University of Minnesota.
- Charles, M.E., Govier, G.W., Hodgson, G.W., 1961. The horizontal pipeline flow of equal density oil–water mixtures. *Canadian Journal of Chemical Engineering* 39, 27–36.
- Feng, J., Huang, P.Y., Joseph, D.D., 1995. Dynamic simulation of the motion of capsules in pipelines. *Journal of Fluid Mechanics* 286, 201–227.
- Joseph, D.D., Renardy, Y.Y., 1993. *Fundamentals of Two-Fluid Dynamics*. Springer, New York.
- Oliemans, R.V.A., Ooms, G., Wu, H.L., Duijvestijn, A., 1986. Core-annular oil/water flow: the turbulent-lubricating-film model and measurements in a 5 cm pipe loop. *International Journal of Multiphase Flow* 13, 23–31.
- Taitel, Y., Dukler, A.E., 1976. A model for predicting flow regime transitions in horizontal and near horizontal gas–liquid flow. *AIChE Journal* 22, 47–55.
- Wallis, G.B., 1969. *One-Dimensional Two-Phase Flow*. McGraw-Hill, New York.
- Wallis, G.B., Dobson, J.E., 1973. The onset of slugging in horizontal stratified air–water flow. *International Journal of Multiphase Flow* 1, 173–193.
- Whitham, G.B., 1974. *Linear and Nonlinear Waves*. Wiley, New York.